Table 1 Radiation characteristics of the receiving systems, received power, and calculated radiation intensities

Antenna	Bandwidth Δf (GHz)	Gain (db)	Average wavelength (cm)	Aperture (cm^2)	Signal (mv)	Detector power P (mw)	Poynting flow P/aperture ($\mu W/cm^2$)	Radiated power in $\Delta\omega$ (mw)	Radiated power (mw/GHz)
Spiral	0.5– 1.0	5	40	400	50–100	0.22 –0.44	0.55– 1.1	15– 30	30 –60
Spiral	1.0– 2.0	5	20	100	50–200	0.22 –0.88	0.55– 2.2	15– 60	15 –60
Spiral	2.0–18.0	3	9	12.9	25– 50	0.156–0.312	12 –24	340–680	21 –42
Horn	3.5– 8.0	20	6	300	50–150	0.312–0.936	1 – 3	28– 84	6.2–18.6
Horn	6.0–12.0	20	3.3	100	25– 50	0.156–0.312	1.6 – 3	45– 84	7.5–14

is first noted, as in Table 1, for each receiving system. The radiation pulse for each receiver has roughly the same shape although there is variation from shot to shot in this waveform for each receiver. Both the amplitude and shape vary but the timing is essentially the same. The variation in peak amplitude is characterized by giving a range of signal strengths in the table. These strengths are converted to received power using the calibrated detector sensitivities, and to received Poynting flux by dividing by the average aperture.

To convert the measured Poynting flux to a radiated power P_{rad} we need the gain G_t of the "transmitting antenna,"

$$(P_{rad}/4\pi r^2)G_t = P_{rec}/A$$

where P_{rec} is the detected or received power in Table 1. Since the radiation is assumed to emanate from random collisions by particles accelerated along the direction of the arc, it is assumed that the pattern is like that of a dipole oriented along the arc. Since the electrodes reflect the signals somewhat, there is a forward focusing affect which enhances the dipole gain (1.5), so we assume $G_t = 2$ consistent with crude observations of the pattern. The total radiated power is then calculated and converted to power density by dividing by the system bandwidth.

Two previous studies of the RFI on these thrusters gave little information on the physical origins of the noise but bear on our results here. The first, a measurement by R. Dolbec[6] of the radiated power at 8 GHz into a 100 MHz band is in good agreement with the power density of Table 1. The present results show a density of 6–60 mw into a 1 GHz band, the variation being a measure of our accuracy as well as variation in power density. Dolbec finds 4.5 dbm in the 100 MHz band (28 mw in 1 GHz). The second study, a short preliminary effort at the Jet Propulsion Lab. by Whittlesey and Beran,[7] gave information on the type of signal and strength. The JPL report showed first that the received power was linear with bandwidth from 5 MHz to about 1 MHz, below which the variation was proportional to the square root of power. The transition is a consequence of the 1 μsec pulse duration and of their "peak and hold" detection system. Above a few MHz the linear dependence verifies the "white noise" or impulse noise behavior observed in the present study and predicted by the theory which follows. They found, further, that the spectrum was approximately flat between 1–8 GHz, and that the fluctuation from shot to shot could be as great as 20 db. This fluctuation is not surprising if the radiation is associated with a process as random as the initial breakdown of the gap. Finally, they found a spectral density for the "average" shot of approximately 6.2 dbm/100 MHz assuming $G_t = 1$, or 21 mw/GHz for $G_t = 2$, agreeing well with the data here.

One last measurement of spectral density was made using a crossed dipole antenna with a broadband (200–400 MHz) hybrid coupler to phase the two dipoles by 90°. The signal was detected with a spectrum analyzer swept very slowly to record each pulse on a long persistence screen. The spectrum was again flat over the range 200–400 MHz at a value within the 6–60 mw/GHz range just quoted.

Several theoretical models were considered to explain the intensity. All assume very short collision times, hence, spectral densities which are constant to frequencies $f_{max} = 10^{16}$–10^{18} Hz. None of these can explain the observed power density $dP/d\omega = 10^{-11}$ joules/Hz. Bremsstrahlung radiation by electron ion collisions gives $\approx 10^{-19}$. X-ray production converts $\sim 1.5 \times 10^{-4}$ of the incident beam power to radiation (with a flat spectrum to 10^{18} Hz), giving $\approx 10^{-15}$ joules/Hz.

Thus, none of the preceding models explain the intensity. One remaining explanation lies in plasma instabilities driven by the incident beam. The spectrum of such instabilities would not extend to the extreme frequencies considered here, hence, the total radiated power is a much smaller fraction of the input power, *Vi*, than is inferred by the collisional models. All the above models imply nearly 100% conversion of beam energy to radiation, which speaks strongly for other mechanisms. Unfortunately, the radiation resulting from instabilities is nearly impossible to calculate, although beam-plasma instabilities generally produce radiation in a broadband up to the electron plasma frequency (3000 GHz) at intensities well above thermal, blackbody, or collisional levels.

References

[1] Guman, W. J. and Peko, P. E., "Solid-Propellant Pulsed Plasma Microthruster Studies," *Journal of Spacecraft and Rockets*, Vol. 5, No. 6, June 1968, p. 732.

[2] Guman, W. J. and Nathanson, D. M., "Pulsed Plasma Microthruster System for Synchronous Orbit Satellite," *Journal of Spacecraft and Rockets*, Vol. 7, No. 4, April 1970, p. 409.

[3] Vondra, R., Thomassen, K. I., and Solbes, A., "Analysis of Solid Teflon Pulsed Plasma Thruster," *Journal of Spacecraft and Rockets*, Vol. 7, No. 12, Dec. 1970, p. 1403.

[4] Vondra, R., Thomassen, K. I., and Soldes, A., "A Pulsed Electric Thruster for Satellite Control," *Proceedings of IEEE*, Vol. 59, 1971, p. 271.

[5] Thomassen, K. I. and Vondra, R. J., "Exhaust Velocity Studies of a Solid Teflon Pulsed Plasma Thruster," *Journal of Spacecraft and Rockets*, Vol. 9, No. 1, Jan. 1972, p. 61.

[6] Dolbec, R. E., "RFI Measurements on a LES-7 Prototype Pulsed Plasma Thruster," *Journal of Spacecraft and Rockets*, Vol. 7, No. 7, July 1970, p. 889.

[7] Wittlesey, A. C. and Beran, E. W., private communication, Aug. 1971, JPL Internal Memo, Pasadena, Calif.

Cold-Plate Design Analysis for Electronic Equipment

EUGENE D. VEILLEUX*

RCA Corporation, Burlington, Mass.

Nomenclature

A = duct cross-sectional area, in.^{2}
C_P = specific heat of fluid, w-min/lb-°C
D = equivalent duct diameter (in.) = $4A/P$

h = heat-transfer film coefficient, w/in.^{2}-°C
k = thermal conductivity of fluid, w/in.-°C
L = duct length, in.
Nu = Nusselt number = hD/K
Pr = Prandtl number = $C_P\mu/K$
Re = Reynolds number = $DV\rho/\mu$
P = duct perimeter, in.
V = velocity of fluid, in./sec
ρ = density of fluid, lb/ft^3
μ = dynamic viscosity of fluid, lb/hr-ft

IN the design of cold plates the heat-transfer film coefficient is dependent on the boundary layer built up at the surface of the internal passage wall of the cold plate, and is a function of the physical and mechanical parameters of the coolant and the physical configuration of the duct through which the coolant flows. The Nusselt number (Nu) is the term containing the heat-transfer film coefficient parameter. In order to properly evaluate the heat-transfer coefficient, the Nusselt number correlates the coolant and duct parameters in a product of Prandtl number (Pr) and Reynolds number (Re). Sieder and Tate[1] generally define this combination of parameters as

$$Nu = f(PrReD/L)^n \tag{1}$$

where f and n are empirically determined constants.

For fully developed flow and small temperature changes between coolant and duct wall, their experimentation resulted in a modification of the original Graetz-Nusselt theory and produced an empirical correlation of the form

$$Nu = 1.86(RePrD/L)^{1/3} \tag{2}$$

Other researchers have performed similar experimentation. One whose work has provided another formula for average heat-transfer film coefficient is Hausen.[2] His empirical correlation has the form

$$Nu = 3.65 + \frac{0.0668(D/L)PrRe}{1 + 0.04[(D/L)PrRe]^{2/3}} \tag{3}$$

A review of a graphical presentation of these equations in Ref. 1 shows that one can expect an approximate variation of up to 25% when fully developed laminar† flow is assumed for a given L/D. By definition, fully developed flow is considered achieved when both the velocity and temperature profiles of the bulk fluid within the duct have reached a parabolic shape. Unfortunately, when a high Prandtl number fluid is utilized, fully developed laminar flow does not occur immediately when fluid enters the heated or cooled section of a duct. Usually, a velocity profile establishes itself in a very short duct length while the temperature profile requires a considerable duct length to become established. Because of the increased turbulence in the boundary layer under this condition, one would expect the heat-transfer coefficient to be larger than it would normally be for fully developed flow. Thus, in the real world of design engineering, the utilization of the preceding formulas in the design of a cold-plate heat exchanger would leave one to wonder how conservative or realistic the design would actually turn out. In an effort to alleviate some of the conservative design practice that usually results, consider an example where a cold plate is to be designed to remove 150 w from electronic black boxes attached to its surfaces. The coolant within the cold plate is to be Coolanol 35[3] flowing at a rate of ½ gal/min and at an inlet temperature of 30°C. The approximate total length of cold plate duct is 71 in. and its cross-sectional configuration is ¾ in. by 1/16 in. A layout of the duct can be seen in Fig. 1. Performing the necessary calculations reveals a Reynolds number of 363, a Prandtl number of 118, and an L/D ratio of 615 if the duct length is 71.0 in. long. If the duct is only considered to have a 16.625-in. length, then the L/D ratio drops to 144. This L/D variation superimposed on graphical data of Ref.1 reveals a 65% variation in heat-transfer coefficient. If this variation is added to the variation due to different experimenters [Eqs. (2) and (3)], we conclude that the safety factor in calculating the heat-transfer coefficient for a serpentine duct cold plate can range between 65% and 85% depending on the selection of parameters chosen.

Consider now the utilization of the Hausen formula [Eq. (3)] for fully developed laminar flow in straight tubes with high Prandtl number fluids. Calculation of the average heat-transfer film coefficient for a 16.625-in. length of tube is shown as curve A of Fig. 2 for various flow rates. The reason for the length selected is that the assumption was made that, as the fluid entered the 180° bend of the tube, the boundary layer would be completely disrupted because of turbulence in the passage, and heat transfer would become greater in this area. As the fluid entered the next straight section, the boundary layer would again be built up and the heat-transfer film coefficient would again approximate what it was in the first straight section and would remain at this value until it entered the second bend. This process would continue to occur throughout the plate resulting in a given mean heat-transfer film coefficient throughout the plate for a particular flow rate. Consideration was also given to a straight tube having a length of 71.0 in. This is shown as curve B on Fig. 2 and assumes that we have a straight duct where the boundary layer is not broken as the fluid makes the 180° bend. This results in a lower heat-transfer film coefficient because the turbulent effect of the bends and the rebuilding of the boundary layer are neglected. These data show that the variation due to duct length previously assumed continues to persist as long as we have fully developed laminar flow. These curves consider that both the velocity profile and temperature profile of the fluid have been developed. It has been found, however, that when a fluid has a high Prandtl number ($Pr > 20$) the length of duct required for the temperature profile to become similar to the velocity profile is large. For this application (½ gal/min), calculations show that the length to develop the temperature profile is approximately 521 in. while the length to develop the velocity profile approximates 5.5 in. As a result, it appears that fully developed laminar flow will never occur in this cold plate because the over-all duct length is shorter than the duct length required to develop the temperature profile. Thus, the accurate estimation of a heat-transfer film coefficient for design purposes is further complicated.

Test Program

A test program was established to evaluate the possible variations in heat-transfer coefficient just discussed. An aluminum cold plate was fabricated and instrumented with thirteen No. 30 B & S (0.010 diam) copper-constantan thermocouples. Thermocouples were located on both sides of the cold plate at the midpoint of each duct and at each bend. Two thermocouples were also located at the inlet and outlet fittings of the cold plate. Cold plate was suspended in a hot water bath to simulate an isothermal heat source, and Coolanol 35 fluid held at a constant temperature was circulated through cold plate. The test data showed a uniform cold plate surface temperature at its center, and a slightly lower surface temperature in the area of 180° bends. These temperature variations indicated an increased local heat-transfer film coefficient in this area, and also suggested a disruption of the boundary layer on the 180° bend.

Received February 7, 1973; revision received April 26, 1973. The author acknowledges that this study was initiated while employed by Sanders Associates, Inc., Nashua, N.H.

Index category: Boundary Layers and Convective Heat Transfer —Laminar.

* Engineering Scientist, Aerospace Systems Division.

† Laminar flow is assumed to exist when the Reynolds numbers is less than 2100.

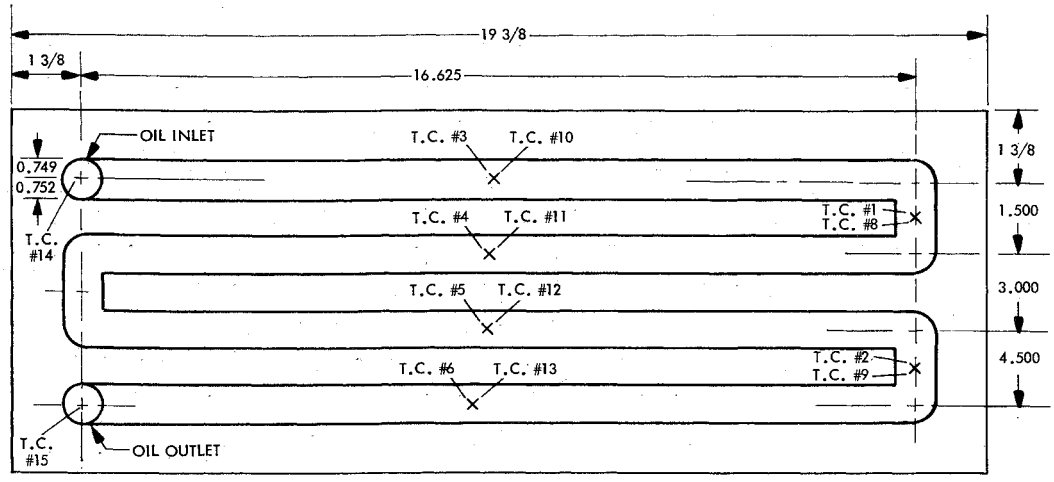

NOTE: THERMOCOUPLES #1 THROUGH 8 ATTACHED TO ONE SIDE OF PLATE. THERMOCOUPLES #9 THROUGH 13 ATTACHED TO OTHER SIDE OF PLATE. THERMOCOUPLES #14 AND 15 ATTACHED TO HYDRAULIC FITTINGS.

OIL DUCT DEPTH = 0.062
OIL DUCT LENGTH = 71.0

T.C. #	T (°C)	T.C. #	T (°C)
1	37	9	37
2	36.5	10	38
3	38	11	38
4	38	12	37.5
5	38	13	38
6	38	14	29
7	32	15	32
8	36		

TEST DATA

Fig. 1 Test cold-plate layout and test data.

Plotting of data for additional flow rates on Fig. 2 results in curve C representing a duct length of 16.625 in. Further, the data shows that at low fluid rates ($\lesssim \frac{1}{2}$ gal/min) the turbulence within the duct, due to not having fully developed laminar flow, is not considerable, and that the actual heat-transfer film coefficient approximates the average heat-transfer film coefficient as determined by the Hausen equation. With increased flow rate, however, Fig. 2, curve C, shows a divergence of both coefficients and indicates the effects of turbulence are coming into play. With this test data correlation it is now possible to predict with reasonable accuracy what the magnitude of the heat-transfer film coefficient will be for simple cold plates having the form factor described herein.

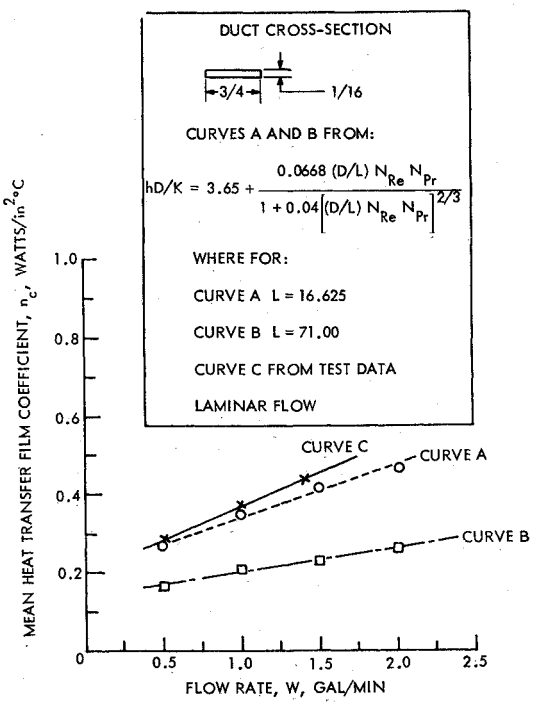

Fig. 2 Film coefficient vs flow rate of Coolanol 35 at 30°C.

References

[1] Grober, H., Erk, S., and Grigull, U., *Fundamentals of Heat Transfer*, McGraw-Hill, New York, 1961, pp. 228–233.

[2] Geidt, W., *Principles of Engineering Heat Transfer*, D. Van Nostrand, Princeton, N.J., 1957, pp. 150–155.

[3] "Dielectric Heat Transfer Fluid for Electronic Equipment," *Technical Bulletin* O/AA-1, April 1, 1967, Monsanto Chemical Co., St. Louis, Mo.

A Nomogram for High-Altitude Plume Structures

JAMES STARK DRAPER* AND EMMETT A. SUTTON*
Aerodyne Research Inc., Burlington, Mass.

Nomenclature

C_F = engine thrust coefficient for actual engine configuration
$C_{F\max}$ = maximum engine thrust coefficient, assuming an infinite area ratio

Received April 13, 1973; revision received June 8, 1973. This work was supported by the Air Force Rocket Propulsion Laboratory under contract FP4511-72-C-0063. The authors wish to express their appreciation for the support and cooperation extended by Capt. S. B. Thompson, the contract monitor.

Index category: Jets, Wakes, and Viscid-Inviscid Flow Interactions.

* Principal Research Scientist. Member AIAA.